

## Three-Wave Mixing with Three Incoming Waves: Signal-Idler Coherent Attenuation and Gain Enhancement in a Parametric Amplifier

Flavius Schackert, Ananda Roy, Michael Hatridge, Michel H. Devoret, and A. Douglas Stone\*

*Departments of Physics and Applied Physics, Yale University, 15 Prospect Street, New Haven, Connecticut 06511, USA*

(Received 9 December 2012; published 16 August 2013)

We demonstrate the time-reversed process of nondegenerate three-wave parametric amplification from three distinct sources in the fully nonlinear regime using a Josephson amplifier. In the reverse process, coherent attenuation, signal and idler beams destructively interfere in the presence of a pump to generate additional pump photons. This effect is observed through the symmetric phase-dependent amplification and attenuation of the signal and idler beams and, in the depleted pump regime, through the phase-dependent modulation of the amplifier gain, directly probing the enhancement of the pump. Results are found to be in good agreement with theory.

DOI: [10.1103/PhysRevLett.111.073903](https://doi.org/10.1103/PhysRevLett.111.073903)

PACS numbers: 42.65.Ky, 42.65.Yj, 85.25.Cp, 85.25.Dq

Parametric amplification based on three-wave mixing is a fundamental process in electromagnetic signal processing [1], both in the optical and microwave frequency domain. More recently, with the advent of quantum information science, three-wave mixing provides a basic building block for measurements at the single photon level [2,3], where it is crucial that the nonlinear mixing process is purely dispersive. An important class of parametric amplifiers make use of three-wave mixing to amplify incoming signal fields through down conversion of a higher frequency pump field. The amplification process involves an incoming pump photon at angular frequency  $\omega_P$  being split up into outgoing signal and idler photons at frequencies  $\omega_S$  and  $\omega_I$ , respectively, where  $\omega_P = \omega_S + \omega_I$ . It has been known since the early days of nonlinear optics [4] that the three-wave mixing process, at the classical level, is in principle time reversible and phase sensitive. This is most easily seen in the case of three-wave mixing by making the undepleted pump approximation, leading to a linear two-port scattering matrix for signal and idler. Typically a nondegenerate parametric amplifier is operated with only an input at the signal port, leading to phase-preserving amplification with power gain,  $G_0$ . However the  $S$  matrix has two eigenvectors corresponding to inputs on both signal and idler port, with reciprocal eigenvalues given approximately by  $2\sqrt{G_0}$ ,  $1/2\sqrt{G_0}$ , the former corresponding to coherent amplification of signal and idler with power gain  $\approx 4G_0$ , and the latter to coherent attenuation (CA). In CA both signal and idler are imposed with the correct relative phase, and they are coherently combined to the pump frequency, leading to power attenuation  $\approx 1/4G_0$ ; this is the time-reversed process to coherent amplification. Until recently there were no nearly lossless microwave amplifiers which could be well modeled by this simple  $S$  matrix; but the Josephson Parametric Converter (JPC) we use here has been shown to be nearly lossless and quantum limited in performance [5,6]. Coherent attenuation and amplification have been measured for some time in the context of degenerate

“phase-sensitive” optical and microwave amplifiers [7–9] and is important in generating squeezed light [10]. In such cases, however, signal, idler, and pump always arise from the same source, which undergoes cascaded nonlinear processes to produce several coherent inputs and signal and idler beams are usually close in frequency (within the same bandwidth of a resonance or as defined by phase-matching conditions); moreover practical parametric amplifiers are typically operated in the undepleted pump regime, which assures insensitivity to signal input power levels. Recently there has been renewed interest in time reversal in fully nonlinear mixing [11], due to its analogy to time-reversed lasing [12,13], and also due to potential applications in quantum information processing. Here we report the first experiments that demonstrate CA with negligible loss from three *distinct* sources in the fully nonlinear regime of three-wave mixing, opening up many potential applications. In our system the signal and idler modes are resonant with nonoverlapping bandwidths (temporal nondegeneracy) and have frequencies that can be engineered to lie several octaves apart [6]. Signal and idler modes also correspond to distinct resonators and signal and idler tones travel on *different transmission lines* (spatial nondegeneracy).

Coherent attenuation requires phase stability of sources, but not entanglement of pairs of photons in different beams. Here we discuss CA at the classical level, but there can also be phase sensitive cancellation of quantum fluctuations, so for compatibility with studies involving quantum noise and entanglement [14,15] we will use here the Hamiltonian or photon description. The coupled mode approach is developed in the Supplemental Material [16]. The Hamiltonian of a three-wave mixing device [17,18], under the rotating wave approximation (RWA), neglecting external drive and signal fields, is

$$H^{\text{RWA}} = \hbar\omega_a a^\dagger a + \hbar\omega_b b^\dagger b + \hbar\omega_c c^\dagger c + \hbar g_3 (a^\dagger b^\dagger c + abc^\dagger), \quad (1)$$

where  $a$ ,  $b$ , and  $c$  are the annihilation operators of the signal, idler, and pump modes of center frequency  $\omega_a$ ,  $\omega_b$ ,  $\omega_c$ , and bandwidth  $\kappa_a$ ,  $\kappa_b$ ,  $\kappa_c$ , respectively, and  $g_3$  is the coupling strength. In this description, the term  $a^\dagger b^\dagger c$ , exploited for amplification (annihilation of a pump photon for the creation of a pair of signal and idler photons), is accompanied by its counterpart  $abc^\dagger$ , which describes CA. We observe this term both by measuring the attenuation of the signal and idler beams when their relative phase is tuned to the CA condition, and, *more directly*, by observing gain increase at the CA point using an additional probe tone. Directly probing the up-converted photons in the pump is very difficult to do in all practical amplifiers, and to our knowledge has not been done in prior experiments.

The Josephson Parametric Converter [5,19] is a widely tunable amplifier, which can be operated as a nondegenerate phase-preserving parametric amplifier [6,20] or as a noiseless frequency converter [21], at GHz frequencies. The JPC, operated at 30 mK in a cryogen-free dilution refrigerator, has three ports [Fig. 1(a)], one each to access

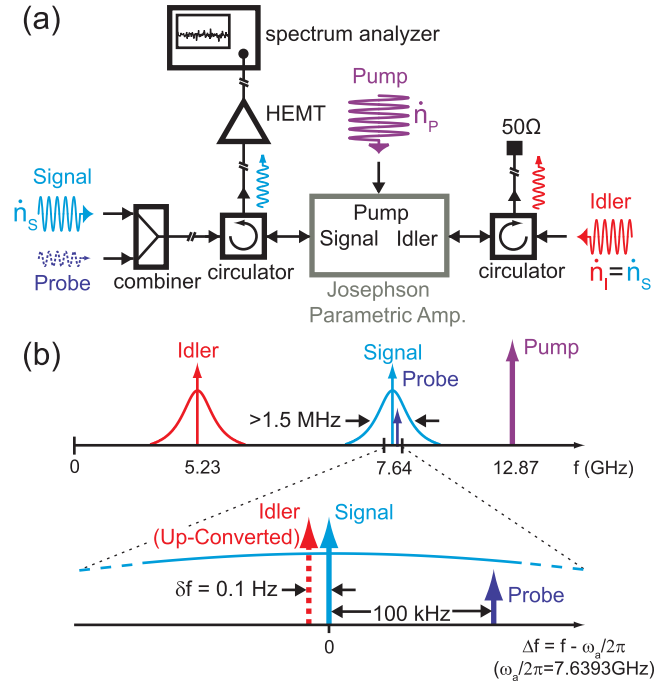


FIG. 1 (color online). (a) Schematic representation of the measurement setup. Four continuous wave (cw) tones are injected in the three ports of the superconducting Josephson parametric amplifier (gray box). Incoming signal, idler, and pump photon fluxes are designated by  $\dot{n}_s$ ,  $\dot{n}_I$ , and  $\dot{n}_p$ , respectively. The output power from the signal port is measured with a spectrum analyzer. (b) Upper: Applied cw tones in frequency space. The horizontal axis is the frequency axis, the colored arrows represent coherent tones, and the Lorentzian shapes represent the gain response function. Lower: enlargement of the signal band. The dashed arrow represents the up-converted idler tone, offset by  $\delta f = 0.1$  Hz from the signal tone, producing a slow variation of the relative phase  $\phi = 2\pi\delta f t$  between signal and idler tones.

the signal (centered around  $\omega_a/2\pi = 7.6393$  GHz), idler (centered around  $\omega_b/2\pi = 5.2277$  GHz), and pump (at  $\omega_c/2\pi = 12.867$  GHz) modes. Cryogenic circulators on the signal and idler ports separate input and output waves, allowing them to travel on different transmission lines (see [6,20] for details on the setup). Four phase-locked microwave generators provide tones to the signal port (signal and probe tones), the idler port (idler tone), and the pump port (pump tone). Incoming signal, idler, and pump photon fluxes are designated by  $\dot{n}_s$ ,  $\dot{n}_I$ , and  $\dot{n}_p$ , respectively. We monitor in time the JPC signal port output power through a spectrum analyzer (SA) set to zero span mode, i.e., set to a frequency window given by the spectrum analyzer's resolution bandwidth (RBW) and center frequency. Specifically to detect the effect of time-reversed mixing in the pump we add a small amplitude probe tone offset from the JPC signal center frequency by 100 kHz [Fig. 1(b)], which allows its detection with the SA without contamination from the large amplitude signal tone at the center of the JPC signal band, as long as the RBW of the SA is set to be much smaller than 100 kHz.

Both the signal and the probe tone are well within the amplification bandwidth of the JPC, which is 1.5 MHz at a gain of 25 dB, and which increases at smaller gains according to the gain bandwidth product  $\sqrt{G_0}B = \pi^{-1}/(\kappa_a^{-1} + \kappa_b^{-1})$  [17], where  $G_0$  is the power gain and  $B$  the dynamical amplification bandwidth (in Hz). In this device  $\kappa_a \approx \kappa_b$ .

First we observe the CA effect in the undepleted regime, where the effect of the upconverted signal and idler photons is negligible. Thus we simply inject coherent signal and idler tones (with no probe tone) and vary their relative phase until they destructively interfere, leading to a strong attenuation of the corresponding output tones by a factor determined by the gain of the amplifier. The effect is described by the linear two-port scattering matrix of the undepleted pump approximation: From the reduced JPC scattering matrix [17]

$$S = \begin{pmatrix} \sqrt{G_0} & -ie^{-i\varphi_p}\sqrt{G_0-1} \\ ie^{i\varphi_p}\sqrt{G_0-1} & \sqrt{G_0} \end{pmatrix}, \quad (2)$$

where  $G_0$  is the (undepleted) gain of the amplifier and  $\varphi_p$  is the pump phase, which we set equal to  $\pi/2$  for convenience. However, it should be emphasized that CA is a *three-wave*, nonlinear interference effect, and can be modulated with the pump phase [22] as well as the relative phase of signal and idler [4]. The eigenvalues of this  $S$  matrix are reciprocals:  $\lambda_{\pm} = \sqrt{G_0} \pm \sqrt{G_0-1}$ , leading to power gain  $4G_0$ ,  $(4G_0)^{-1}$ , respectively, at large gains. If  $A$  is the signal amplitude ( $\dot{n}_s = |A|^2$ ), the eigenvectors are  $\vec{e}_+ = (A, -A)$ ,  $\vec{e}_- = (A, A)$ , requiring a balanced idler input ( $\dot{n}_I = \dot{n}_s$ ), either in phase or  $\pi$  out of phase.

If balanced beams with relative phase  $\phi$  are input, the normalized output power,  $P = P_{\text{out}}/(G_0 P_{\text{in}})$ , (where  $P_{\text{out}}$ ,  $P_{\text{in}}$  are the signal output and input power) is given by

$$P = 2 - G_0^{-1} - 2\sqrt{1 - G_0^{-1}} \cos\phi, \quad (3)$$

which varies between  $P \approx 4$  for  $\phi = \pi$  and  $P \approx (4G_0^2)^{-1}$  for  $\phi = 0$  (CA). As the amplifier approaches the oscillation threshold,  $G_0 \rightarrow \infty$  and the cancellation becomes perfect [11]. As noted above, this effect is similar to the time-reversed laser operation in a coherent perfect absorber [12,13].

To observe CA in the JPC we slowly vary the phase  $\phi$  between signal and idler input tones at a rate of 0.1 Hz, by offsetting the idler tone above the JPC idler mode center frequency by  $\delta f = 0.1$  Hz. The parametric amplification process up-converts and amplifies the idler tone, which, as a result of the detuning, appears  $\delta f$  below the amplified signal tone. To be able to monitor the power at the signal port in time with sufficient resolution of the phase  $\phi = 2\pi\delta f t$ , we set the SA to a RBW that is faster than the detuning  $\delta f$ : 36 Hz when observing the attenuation of the signal tone and 51 Hz when monitoring the probe gain [23] (see Supplemental Material at [16] for choice of bandwidths and detunings).

Figure 2 shows the CA of the input signal tone, for signal and idler input powers well below (at least 10 dB) the 1 dB amplifier compression point [24]. The light blue trace is the measured, normalized signal output power  $P$ , as function of the relative phase  $\phi$  between signal and idler. In addition, the data are fit to Eq. (3) which is then plotted as the overlaid white curve; the single fit parameter,  $G_0 = 11$  dB agrees with its independently measured value. As noted, at large gains, and  $\phi = (2n+1)\pi$ ,  $n \in \mathbb{Z}$ , constructive interference yields an increased output 6 dB (factor of 4) above the signal output power with idler tone off ( $G_0 P_{in}$ , pink trace), while CA occurs  $\phi = 2\pi n$ , when only a fraction  $(4G_0)^{-1}$  of the incident power leaves the JPC through the signal and idler ports [normalized power  $P = (4G_0^2)^{-1}$ ].

The data in the inset in Fig. 2(a) show  $P$  for increasing  $G_0$ , confirming this behavior.

The coherent attenuation is a measure of the efficiency of the conversion of signal and idler photons into pump photons. Figure 2(b) shows that there is good agreement between our data (blue dots) and the prediction of Eq. (3) (red) for all gains up to the experimental limit imposed by the system noise floor [black triangles; see arrow labeled “dist. to NF” in Fig. 2(a)]. All error bars are calculated from the noise floor data according to the Dicke radiometer formula [25]. The increase for the CA data at larger gains is due to the fact that we systematically decrease the signal and idler tone powers at larger gains to make sure to stay well below the saturation point of the device (we keep  $G_0 \dot{n}_S$  approximately constant while ensuring that we exactly have  $\dot{n}_S = \dot{n}_I$ ). This leads to a decrease in signal-to-noise ratio, as the JPC noise (and thus the system noise) increases with  $G_0$ . A more serious limitation to the CA measurement is the fact that the noise floor [black trace in Fig. 2(a)] is pushed up when  $G_0$  increases, while the input

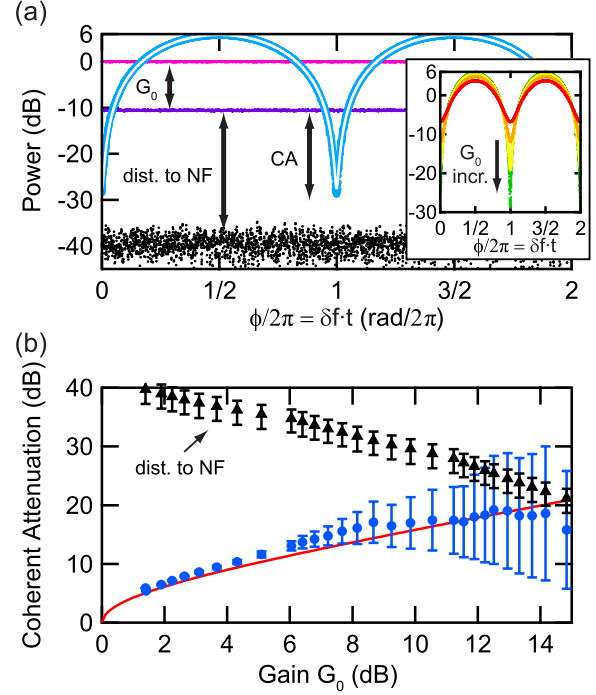


FIG. 2 (color online). (a) Normalized output power as a function of  $\phi$  (light blue) and fit to Eq. (3) (white), for balanced signal and idler incoming photon fluxes ( $\dot{n}_S = \dot{n}_I$ ) and  $G_0 = 11$  dB. Calibration traces are as follows: idler turned off (pink); idler and pump off (purple); signal and idler off (i.e., noise floor, black). Arrows indicate how various quantities [gain ( $G_0$ ), coherent attenuation, distance of zero cancellation to noise floor (dist. to NF)] are measured. Inset: shown traces correspond to gains varying from 1 (red) to 11 dB (green). (b) Magnitude of CA versus gain at maximum interference point (blue). Red solid trace represents the theory, and the black triangles the resolution limitations due to the finite distance to the noise floor.

signal is adjusted to decrease. This means that our ability to observe the CA effect decreases for increasing gains [see “dist. to NF” in Fig. 2(b)]. We could reduce RBW and hence the noise floor, but the trade-off in phase resolution is not favorable.

The coherent attenuation effect on the signal and idler tone as described by Eq. (3) is easily calculated in the undepleted pump approximation, but it is more general and still applies to the fully nonlinear regime of larger signal and idler relative to the pump. In this case coherent amplification will reduce the gain of the amplifier for additional tones, since the signal and idler are significantly reducing the pump, while CA will actually *enhance* the gain over its undepleted value. Hence we enter a new regime of phase-dependent gain modulation. This gain modulation provides a method to confirm that the attenuated signal and idler photons at the CA condition are not lost to some other dissipative process but are being coherently converted to pump photons, which can amplify an additional probe tone that we now introduce.

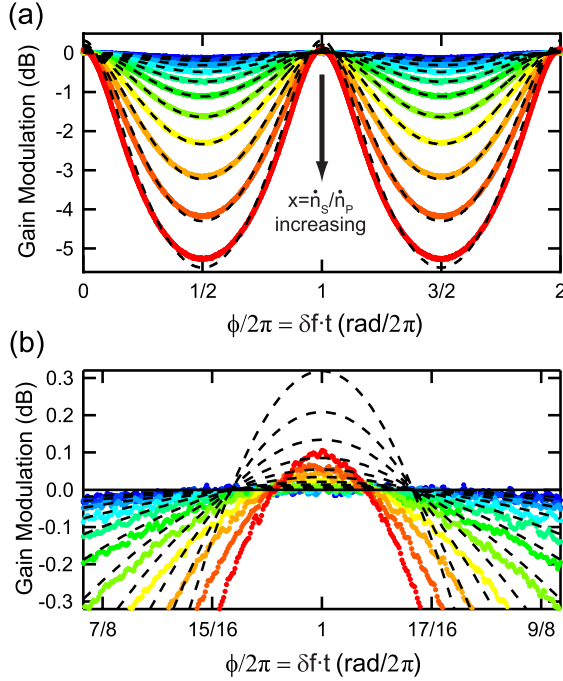


FIG. 3 (color online). (a) Phase-dependent depletion of signal port gain ( $G_0 = 11$  dB). Amplified probe power is measured in a 51 Hz RBW (signal tone is offset by 100 kHz). Traces correspond to signal and idler photon fluxes increasing by 2 dB (from blue to red). Dashed lines are least square fits of gain modulation theory. (b) Enlargement of the region around  $\phi = 2\pi$ . Gain enhancement above  $G_0 = 11$  dB (0 dB line) is clearly visible for experimental data.

Experimentally, we keep the signal and idler photon fluxes equal ( $\dot{n}_s = \dot{n}_i$ ) but in contrast to the experiment of Fig. 2, with signal and idler amplitudes large enough to significantly saturate the device. Equation (3) must be generalized, with the undepleted gain,  $G_0$  being replaced by a nonlinear gain,  $G = G(\phi, x)$ ,  $x = \dot{n}_s/\dot{n}_p$ , which must be calculated self-consistently (see Supplemental Material [16]). Figure 3(a) shows the expected large modulation of the gain with  $\phi$ , and, most dramatically, around  $\phi = 2\pi$  [see Fig. 3(b)], we observe an *increase* in the JPC gain; moreover, the gain enhancement increases as we increase  $x$  in 2 dB steps (colors from blue to red). The data set shown corresponds to an undepleted gain of 11 dB (normalized to 0 dB line), and an applied pump power that is not changed across traces. Note that the gain enhancement  $\sim x$ , whereas the gain reduction  $\sim 4G_0x$ , so the large asymmetry between the two effects is expected.

The dashed lines in Fig. 3 correspond to theory with a single fit parameter  $x$ . As expected, the fits reproduce the 2 dB steps of applied signal and idler powers (not shown). We find excellent agreement between our theory and our experiment for phases  $\phi$  away from  $2\pi n$ , where signal and idler fields constructively interfere and lead to a depletion of the pump photon flux, manifested as a decrease of the JPC gain.

Although the maximum experimental value at  $\phi = 2\pi$  is about 1/3 of the expected theoretical value [16], we unambiguously observe significant gain enhancement in our JPC, the key signature of the coherent conversion of signal and idler photons into pump photons. There are several reasons for the discrepancy between experimental and theoretical gain enhancement: the experiment requires significant averaging with the given bandwidths and powers (ultimately limited by the JPC dynamical bandwidth and dynamic range), while each modulation is rather slow (0.1 Hz). It is thus sensitive to 1/f noise and microwave generator phase drifts. Further, any mismatch between  $\dot{n}_s$  and  $\dot{n}_i$  decreases the gain enhancement. Finally, there may be a contribution due to spurious dissipation in the CA process.

The presented gain enhancement results can be understood as a benchmark for the level of control we have over all degrees of freedom in our three-wave mixing device. Any hidden (uncontrolled) degree of freedom other than the signal, idler, and pump modes will inevitably be perceived as dissipation and thus lead to a reduction in the gain enhancement effect. A potential application for the operation of a JPC in the attenuating mode is its use in phase-locking two coherent tones of different frequencies in a feedback loop, which could be crucial for quantum information processing with artificial atoms.

Discussions with Hui Cao are gratefully acknowledged. This research was supported by IARPA under Grant No. W911NF-09-1-0369, ARO under Grant No. W911NF-09-1-0514 and NSF under Grants No. DMR-1006060 and No. DMR-0653377. A. D. S. acknowledges support by NSF under Grant No. ECCS-1068642. Facilities used were supported by Yale Institute for Nanoscience and Quantum Engineering and NSF MRSEC DMR 1119826.

\*douglas.stone@yale.edu

- [1] P. A. Franken, A. E. Hill, C. W. Peters, and G. Weinreich, *Phys. Rev. Lett.* **7**, 118 (1961).
- [2] A. Aspect, P. Grangier, and G. Roger, *Phys. Rev. Lett.* **47**, 460 (1981).
- [3] P. G. Kwiat, K. Mattle, H. Weinfurter, A. Zeilinger, A. V. Sergienko, and Y. Shih, *Phys. Rev. Lett.* **75**, 4337 (1995).
- [4] J. A. Armstrong, N. Bloembergen, J. Ducuing, and P. S. Pershan, *Phys. Rev.* **127**, 1918 (1962).
- [5] N. Roch, E. Flurin, F. Nguyen, P. Morfin, P. Campagne-Ibarcq, M. H. Devoret, and B. Huard, *Phys. Rev. Lett.* **108**, 147701 (2012).
- [6] N. Bergeal, F. Schackert, M. Metcalfe, R. Vijay, V. E. Manucharyan, L. Frunzio, D. E. Prober, R. J. Schoelkopf, S. M. Girvin, and M. H. Devoret, *Nature (London)* **465**, 64 (2010).
- [7] M. A. Castellanos-Beltran and K. W. Lehnert, *Appl. Phys. Lett.* **91**, 083509 (2007).

- [8] J. Kakande, C. Lundström, P.A. Andrekson, Z. Tong, M. Karlsson, P. Petropoulos, F. Parmigiani, and D.J. Richardson, *Opt. Express* **18**, 4130 (2010).
- [9] T. Umeki, O. Tadanaga, A. Takada, and M. Asobe, *Opt. Express* **19**, 6326 (2011).
- [10] R.E. Slusher, L.W. Hollberg, B. Yurke, J.C. Mertz, and J.F. Valley, *Phys. Rev. Lett.* **55**, 2409 (1985).
- [11] S. Longhi, *Phys. Rev. Lett.* **107**, 033901 (2011).
- [12] Y.D. Chong, L. Ge, H. Cao, and A.D. Stone, *Phys. Rev. Lett.* **105**, 053901 (2010).
- [13] W. Wan, Y. Chong, L. Ge, H. Noh, A.D. Stone, and H. Cao, *Science* **331**, 889 (2011).
- [14] E. Flurin, N. Roch, F. Mallet, M.H. Devoret, and B. Huard, *Phys. Rev. Lett.* **109**, 183901 (2012).
- [15] N. Bergeal, F. Schackert, L. Frunzio, and M.H. Devoret, *Phys. Rev. Lett.* **108**, 123902 (2012).
- [16] See Supplemental Material at <http://link.aps.org/supplemental/10.1103/PhysRevLett.111.073903> for a comparison of the experimental gain enhancement to the theoretical prediction as a function of  $x$  at gains of 11 and 15 dB.
- [17] N. Bergeal, R. Vijay, V.E. Manucharyan, I. Siddiqi, R.J. Schoelkopf, S.M. Girvin, and M.H. Devoret, *Nat. Phys.* **6**, 296 (2010).
- [18] B. Abdo, A. Kamal, and M. Devoret, *Phys. Rev. B* **87**, 014508 (2013).
- [19] M. Hatridge, S. Shankar, M. Mirrahimi, F. Schackert, K. Geerlings, T. Brecht, K.M. Sliwa, B. Abdo, L. Frunzio, S.M. Girvin, R.J. Schoelkopf, and M.H. Devoret, *Science* **339**, 178 (2013).
- [20] B. Abdo, F. Schackert, M. Hatridge, C. Rigetti, and M. Devoret, *Appl. Phys. Lett.* **99**, 162506 (2011).
- [21] B. Abdo, K. Sliwa, F. Schackert, N. Bergeal, M. Hatridge, L. Frunzio, A.D. Stone, and M. Devoret, *Phys. Rev. Lett.* **110**, 173902 (2013).
- [22] C. Kim, R.-D. Li, and P. Kumar, *Opt. Lett.* **19**, 132 (1994).
- [23] We chose to present these two data sets as this is where we best achieved the balance between signal and idler photon flux.
- [24] D. Pozar, *Microwave Engineering* (Wiley, New York, 1997).
- [25] R.H. Dicke, *Rev. Sci. Instrum.* **17**, 268 (1946).